JOC The Journal of Organic Chemistry

Subscriber access provided by BIU Pharmacie | Faculté de Pharmacie, Université Paris V

Article

Self-Assembling [n.n]Paracyclophanes: A Structure–Property Relationship Study

Will R Henderson, Yu Zhu, Danielle E Fagnani, Guancen Liu, Khalil A. Abboud, and Ronald K Castellano

J. Org. Chem., **Just Accepted Manuscript** • DOI: 10.1021/acs.joc.9b03120 • Publication Date (Web): 11 Dec 2019

Downloaded from pubs.acs.org on December 11, 2019

Just Accepted

"Just Accepted" manuscripts have been peer-reviewed and accepted for publication. They are posted online prior to technical editing, formatting for publication and author proofing. The American Chemical Society provides "Just Accepted" as a service to the research community to expedite the dissemination of scientific material as soon as possible after acceptance. "Just Accepted" manuscripts appear in full in PDF format accompanied by an HTML abstract. "Just Accepted" manuscripts have been fully peer reviewed, but should not be considered the official version of record. They are citable by the Digital Object Identifier (DOI®). "Just Accepted" is an optional service offered to authors. Therefore, the "Just Accepted" Web site may not include all articles that will be published in the journal. After a manuscript is technically edited and formatted, it will be removed from the "Just Accepted" Web site and published as an ASAP article. Note that technical editing may introduce minor changes to the manuscript text and/or graphics which could affect content, and all legal disclaimers and ethical guidelines that apply to the journal pertain. ACS cannot be held responsible for errors or consequences arising from the use of information contained in these "Just Accepted" manuscripts.

is published by the American Chemical Society. 1155 Sixteenth Street N.W., Washington, DC 20036

Published by American Chemical Society. Copyright © American Chemical Society. However, no copyright claim is made to original U.S. Government works, or works produced by employees of any Commonwealth realm Crown government in the course of their duties.

Self-Assembling [n.n]Paracyclophanes: A Structure–Property Relationship Study

Will R. Henderson, Yu Zhu, Danielle E. Fagnani, Guancen Liu, Khalil A. Abboud, Ronald K. Castellano*

Department of Chemistry, University of Florida, PO Box 117200 Gainesville, FL 32611-7200, USA

KEYWORDS Self-assembly, paracyclophane, planar-chiral, supramolecular polymer, structure–property relationship

ABSTRACT: Reported here is the synthesis, characterization, and isodesmic supramolecular polymerization of [3.3]paracyclophane-5,8,14,17-tetracarboxamide (**[3.3]pCpTA**). The self-assembling monomer, a bridge-expanded homolog of [2.2]paracyclophane-4,7,12,15-tetracarboxamide (**[2.2]pCpTA**), forms homochiral assemblies in nonpolar solution and the solid state through double helical intermolecular and transannular hydrogen bonding. The additional methylene unit in the [3.3]paracyclophane bridge results in a weakened supramolecular assembly for **[3.3]pCpTA** compared to **[2.2]pCpTA** in solution. Likely origins of the change in assembly strength, revealed through X-ray crystallography, computational analysis, and solution-phase spectroscopy, are an increase in (a) the intramolecular *and* intermolecular deck-to-deck spacing compared to [2.2]paracyclophane resulting from larger amide dihedral angles accompanying transannular hydrogen bonding in the [3.3]paracyclophane, and (b) monomer entropy associated with the scissoring motion of the [3.3]paracyclophane bridge.

INTRODUCTION

Supramolecular polymers are macromolecular structures that are formed through iterative assembly of typically bifunctional monomers through non-covalent interactions.[1-2] The formation of 1-D supramolecular polymers through a combination of hydrogen bonding and π–π interactions from small aromatic monomers has been extensively studied, with structure–property,[3-6] and even structure–mechanism[7-8] relationships being established for privileged monomer families.[9-10] Fundamental studies of supramolecular polymers provide an opportunity to understand how molecular structure changes can rationally, and reversibly, tune material properties. The development of structure–property and structure–mechanism relationships in novel monomer families is critical for informing the next generations of functional supramolecular materials.

In addition to studying the influence of monomer structure, it is important to consider the impact of monomer conformation and dynamics on supramolecular assembly mechanism and thermodynamics. It has been shown that a dichotomy exists between an increase in entropy of conformationally flexible molecular recognition units, and the ability of these units to optimize complementary interactions.[11] Two recent publications from Palmans and Meijer demonstrate that the introduction of conformational flexibility to a supramolecular monomer can lead to changes in cooperativity, chiral amplification, and solvent sensitivity, as well as pathway complexity in assembly.[12-13] Additionally, Yagai demonstrated that an increase in conformational flexibility can lead to off-pathway aggregates as well as changes in cooperativity.[14] Therefore, monomer conformation and dynamics are potentially programmable elements expected to influence not only assembly thermodynamics, but also assembly mechanism.

In 2016, our group reported the synthesis and self-assembly of [2.2]paracyclophane-4,7,12,15-tetracarboxamide

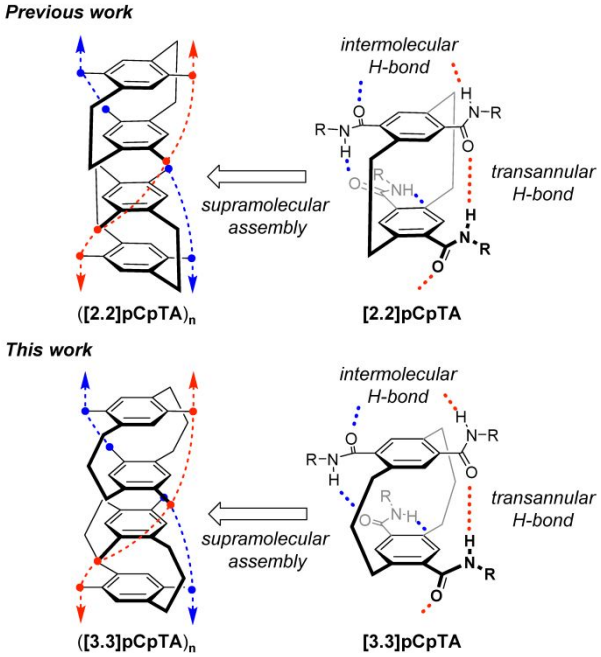

Figure 1. Representation of the hydrogen bond directed self-assembly of **[2.2]pCpTA** and **[3.3]pCpTA**.

(**[2.2]pCpTA**),[15] followed by a computational study to confirm an isodesmic supramolecular polymerization mechanism (Figure 1).[16] The self-complementary molecular recognition unit is created from a chiral arrangement of two pairs of *para*- and pseudo-*ortho* positioned amides on the [2.2]paracyclophane hydrocarbon framework. The design establishes a strong intramolecular (transannular) hydrogen bond that preorganizes the molecule for intermolecular amide hydrogen bonding.[17] The result is a homochiral supramolecular assembly whose helical sense is dictated by the planar chirality (R_p or S_p) of the **[2.2]pCpTA**

monomer; the assemblies persist in the solid-state and in organic solution.

We envision the **[n.n]pCpTAs** as an important class of molecules for establishing structure–property relationships in supramolecular polymers because structural changes can be introduced to the paracyclophane monomer unit without significantly varying the nature of the molecular recognition motif shown in Figure 1. Reported here is a comparison of the hydrogen bond directed assemblies of **[2.2]pCpTA** and the bridge-expanded homologue [3.3]paracyclophane-5,8,14,17-tetracarboxamide (**[3.3]pCpTA**) (Figure 1) that provides insight into how conformational dynamics and subtle monomer structural differences (e.g., an increased deck-to-deck distance) govern paracyclophane self-assembly. The progression from [2.2]paracyclophane (**[2.2]pCp**)[18] to [3.3]paracyclophane (**[3.3]pCp**) is logical given how the two have been compared in the context of charge-transfer complexes,[19-22] multilayered architectures,[23-26] and donor-acceptor chromophore complexes.[27-29] Through a combination of NMR, IR, X-ray, and computational studies, we show that the increase in conformational freedom for **[3.3]pCpTA** leads to an increase in monomer entropy that results in a weaker supramolecular assembly when compared to the more rigid **[2.2]pCpTA**. The findings reported here are expected to be general and should allow for the rational design of new molecular recognition units and supramolecular polymers.

RESULTS AND DISCUSSION

DESIGN

The additional bridge methylene in **[3.3]pCp** decreases the distortion of both the alkyl bridge and the phenyl decks (Figure 2). To wit, the benzene rings in **[2.2]pCp** are bent out of the plane by 12.5° compared to 6.4° in **[3.3]pCp**, and the H_2C–CH_2 bond length of the alkyl bridge is longer in **[2.2]pCp** by 0.10 Å (1.53 Å vs 1.63 Å). The result is a decrease in the overall strain energy of **[3.3]pCp** (11.9 kcal mol^{-1}) compared to **[2.2]pCp** (30.9 kcal mol^{-1})[30] and an increase in conformational flexibility for **[3.3]pCp**.[31]

Although the symmetry of **[2.2]pCp** was a point of controversy,[32-35] it is now accepted that the bridge carbons of **[2.2]pCp** maintain a slight twist (D_2 symmetry) with a minimal barrier to interconversion (ca. 0.2 kcal mol^{-1}).[36-38] As a result, **[2.2]pCp** is conformationally rigid, with only slight skeletal vibrations; this rigidity is expected to persist in the **[2.2]pCpTA** monomer. Conformational complexity in **[3.3]pCp** arises from two major conformers (Figure 2), *cis* (*boat*) and *trans* (*chair*), that are close in energy (the *chair* conformer is +0.17 kcal mol^{-1} relative to *boat*), with a barrier to interconversion of ca. 12 kcal mol^{-1}.[39-41] The decrease in rigidity and increase in conformational freedom for **[3.3]pCpTA**, while maintaining the same molecular recognition motif, provides an opportunity to examine the influence of monomer conformational dynamics on association thermodynamics and consequently supramolecular polymerization in these systems. We expect the enhanced monomer dynamics of **[3.3]pCpTA** to have enthalpic (i.e., steric interactions with amides involved in transannular H-bonding) as well as entropic consequences (increasing the number of energetically accessible monomer states). Transannular hydrogen bonding as an important aspect of the molecular recognition unit, is expected to be sensitive to monomer dynamics changes. Accordingly, changes in the strength or geometry of the transannular H-bond should be reported on by assembly differences.

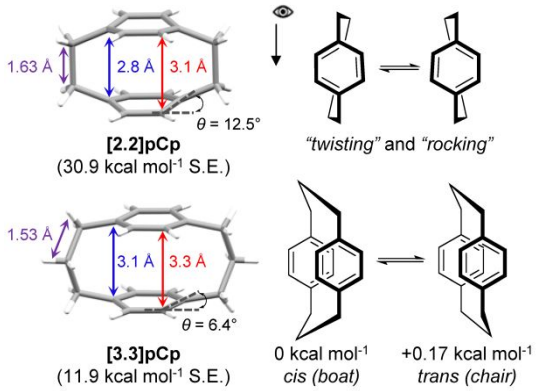

Figure 2. Differences in **[2.2]pCp** (CCDC 1147732, top) and **[3.3]pCp** (CCDC 1229531, bottom) scaffold structures (left), strain energy (S.E.), and conformational dynamics (right).

The additional bridge methylene could also play a role in the kinetics of supramolecular polymerization. Similar to **[2.2]pCpTA**, there are two low energy amide conformers (*syn*- and *anti*-) that differ in the H-bonding directionality of the two pairs of pseudo-*ortho* amides. These conformers are expected to have different assembly thermodynamics and potentially different assembly mechanisms based on differences in H-bonding arrangements and assembly macrodipoles.[16] If the barrier to interconversion between any of the assembling conformers (*syn*- and *anti*- or *boat* and *chair*) becomes high enough for their interconversion to become slow on the experimental timescale, competing assembly pathways could exist.[42]

((±)-2b).

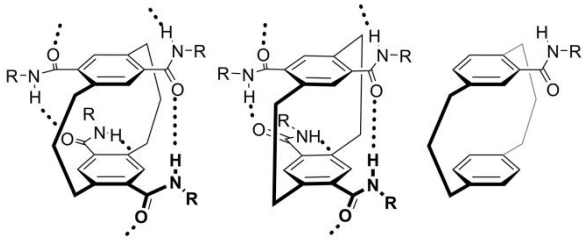

Figure 3. The self-assembling **[3.3]pCpTAs (±)-1a–e**, [**2.2]pCpTAs (±)-2a–b**, and non-assembling **[3.3]pCp**-monoamide **(±)-3** examined in this study.

The molecules explored in this work are shown in Figure 3. Similar to **[2.2]pCpTA**, alkyl groups were incorporated to provide solubility for **[3.3]pCpTA (±)-1**. Hexyl chains were introduced to **[3.3]pCpTA (±)-1a** and the non-assembling **[3.3]pCp**-monoamide **(±)-3** for solution studies, while a derivative with propyl chains **(±)-1b** was utilized for single-crystal X-ray analysis. Due to the limited diffraction of **(±)-1b**, derivatives **(±)-1c–e** were prepared to allow for crystallization and aid in X-ray diffraction. The most crystalline of these, **(±)-1c** with benzyl sidechains, proved best suited for X-ray diffraction. **[2.2]pCpTA**, compound **(±)-2**, was employed to compare self-assembly in nonpolar solutions (**(±)-2a**) and in the solid state.

SYNTHESIS

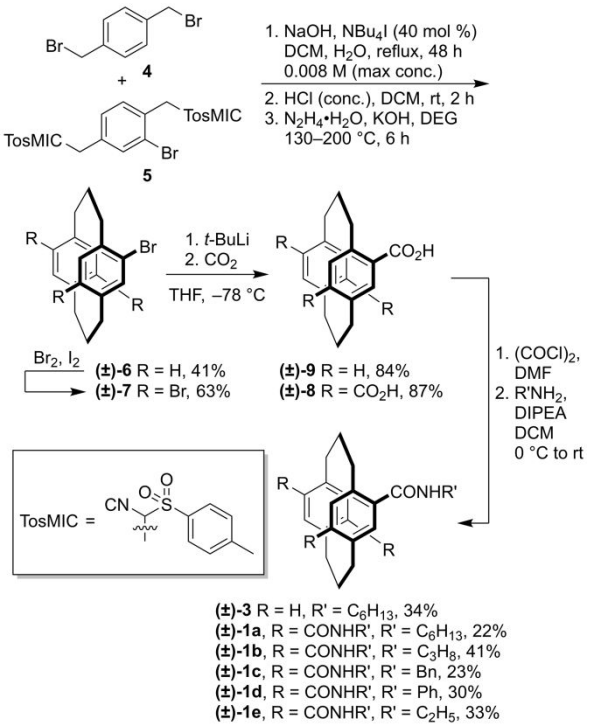

Scheme 1. The synthetic approach to **[3.3]pCpTAs (±)-1a–e** and **(±)-3** from **4** and **5**.

Unlike commercially available **[2.2]pCp**, whose synthetic manipulation is well documented, **[3.3]pCp** is not commercially available and is much less explored synthetically. Synthetic strategies to substituted [n.n]paracyclophanes generally rely on functionalization of the parent cyclophane, or pre-installation of functional groups prior to macrocyclization.[43-45] Various attempts to pre-install all four functional groups (in this case bromine atoms) and cyclize to the substituted **[3.3]pCp** failed, so the strategy was re-evaluated to begin with synthesis of **[3.3]pCp** followed by subsequent functionalization. Initially, we relied on a strategy of synthesizing parent **[3.3]pCp** through toluenesulfonylmethyl isocyanide (TosMIC) macrocyclization chemistry in DMF,[46] and functionalizing it in an analogous manner to the synthesis of **[2.2]pCpTA** (Scheme S1, details in experimental section). Compound **(±)-1a** was successfully prepared on a small scale but the synthesis of **[3.3]pCp** was poorly scalable, which motivated us to pursue an efficient synthesis.

An optimized synthetic route proceeded through a modification of a known literature procedure,[47] involving macrocyclization of 1,4-(bisbromomethyl)benzene (**4**) and bromo-TosMIC adduct (**5**) under phase transfer conditions (Scheme 1). This reaction utilized the increased solubility of **5** in dichloromethane compared to non-brominated TosMIC adduct (Scheme S2, Supporting Info) and proved to be milder, scalable, and more efficient. Hydrolysis of the cyclic tosMIC adduct yielded **[3.3]pCpBr**-diketone (compound **(±)-12**, Supporting Info), which underwent Wolff–Kishner reduction smoothly to yield **[3.3]pCpBr (±)-6**. Bromination of bromo-**[3.3]pCp (±)-6** proceeds much more readily than bromination of **[2.2]pCp**[48] under identical conditions due to the more electron-rich nature of **[3.3]pCp**.[20] Tribromination of **(±)-6** gives desired **[3.3]pCp**-5,8,14,17-tetrabromide **(±)-7** and the undesired **[3.3]pCp**-5,6,14,15-tetrabromide regioisomer which could be separated by silica gel chromatography. Lithium-halogen exchange of **(±)-7** with *t*-BuLi, followed by quenching with gaseous CO_2, yields [3.3]pCp-5,8,14,17-tetracarboxylic acid **(±)-8**. Compound **(±)-8** could be converted to the corresponding acyl chloride with oxalyl chloride and catalytic DMF, followed by condensation with a primary amine to give **[3.3]pCpTA (±)-1** in reasonable yields.

The synthetic approach to monoamide comparator **(±)-3** followed the same carboxylation and amide bond formation approach from **(±)-6**.

X-RAY CRYSTALLOGRAPHY

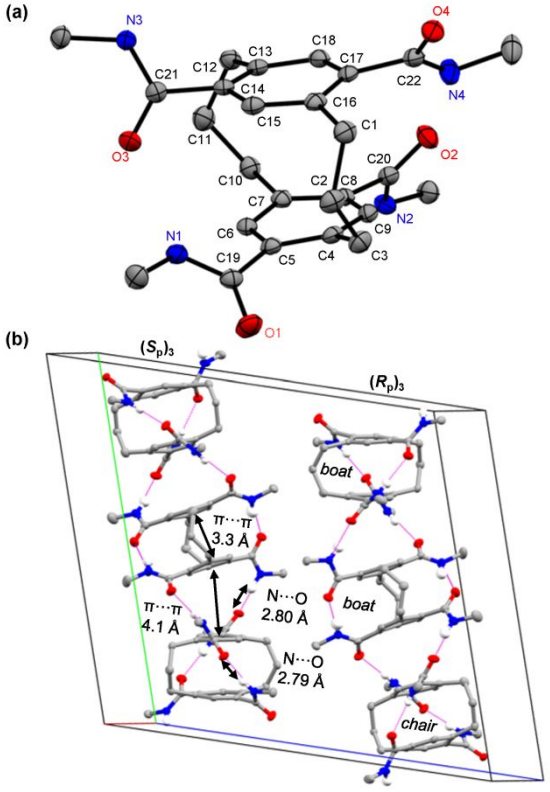

Figure 4. ORTEP of monomeric **(S_p)-1c** in the *boat* conformation (a) and the unit cell (b) featuring homochiral trimers of **(S_p)-1c** (left) and **(R_p)-1c** (right) and their average H-bond (N···O) and π–π (centroid···centroid) distances. Magenta dashed line indicates hydrogen bonding. Atom color code: blue N, gray C, red O, white H. Bridge disorder, benzyl sidechains, ethyl acetate solvent molecules, and hydrogens not involved in H-bonding removed for clarity. Thermal ellipsoids are shown at the 50% probability level.

The introduction of benzyl sidechains **(±)-1c** allowed for the growth of single crystals suitable for X-ray diffraction (slow evaporation of an ethanol/ethyl acetate solution). Homochiral 1-D stacks formed by double-helical hydrogen bonding between *anti*-aligned amides unambiguously confirm the intended **[3.3]pCpTA** assembly design and reflect the wider applicability of the **[n.n]pCpTA** self-assembly motif (Figure 4).[49] The presence of the *anti*- conformer in the crystal structure is consistent with that observed in the crystal structure of **(±)-2b** and with what is predicted based on DFT calculations (M06-2X/6-31+G* level of theory) with the **[3.3]pCpTA** *syn*- monomers being higher in energy by 0.8–1.3 kcal mol^{-1} and the **[3.3]pCpTA** *syn*- dimers being higher in energy by > 6 kcal mol^{-1} (Table S1).

The asymmetric unit is comprised of three configurationally equivalent monomers (**(R_p)-1c** or **(S_p)-1c**) that differ in the conformation of their alkyl bridge. Although there is disorder associated with the central bridge carbon, two molecules of the unit-cell trimer are in the *boat* conformation while the third molecule is in the *chair* conformation. This indicates that some combination of *chair* and *boat* conformers is still present in the solid-state assembly and that *chair/boat* interconversion and association is likely occurring in solution assemblies.

Out of the six amides present in the unit cell, only five are participating in intermolecular hydrogen bonds in the crystal; one amide of the *chair* monomer is not participating in an intermolecular hydrogen bond to the next *boat* monomer (N···C=O distance 5.56 Å). This missing contact is likely a result of crystal packing forces accommodating the bulky benzyl sidechains and leads to less cofacial overlap for the assembly of **(±)-1c** (Figure S31). The average transannular hydrogen bond distances (e.g., $N_1\cdots O_3$) of 2.80 Å are nearly identical to the average intermolecular (N···O) distance of 2.79 Å (Figure 4), and to the values observed in **(±)-2b** (2.81 Å, and 2.77 Å, respectively). Average amide torsional angles ($\phi_1 \approx \phi_3 \approx 49°$ and $\phi_2 \approx \phi_4 \approx -129°$) are larger for **(±)-1c** and show the greater extent to which the amides are twisted out of plane with the aryl rings compared to **(±)-2b** ($\phi_1 \approx \phi_3 \approx 38°$ and $\phi_2 \approx \phi_4 \approx -141°$).

These structural parameters obtained from X-ray crystallography are consistent with values estimated from DFT geometry optimization (Table S1) for the **[3.3]pCpTA** monomer ($\phi_1 \approx \phi_3 \approx 50°$ and $\phi_2 \approx \phi_4 \approx -137°$) with the slight torsional disparity likely a result of optimized intermolecular H-bonding in the crystal. Intermolecular aryl centroid···centroid distances range from 3.9–4.3 Å, slightly longer than the average aryl ring centroid···centroid distances of **(±)-2b** (3.4–3.8 Å) and those predicted by DFT calculations of the dimers (3.7 Å). The longer intermolecular π–π distances in **[3.3]pCpTA** are a result of the larger amide dihedral angles (i.e., C_6–C_5–C_{19}–O_1) needed to maintain optimal transannular H-bonding across an increased deck-to-deck distance (3.3 Å in **(±)-1c** compared to 3.1 Å in **(±)-2b**) prior to intermolecular H-bonding.

SOLUTION STUDIES

Variable concentration (0.1–30 mM) ^{1}H NMR solution studies in $CDCl_3$ (Figure 5a) show a deshielding of the amide N–H resonance (H_a/H_b) and a shielding of the Ar–H resonance (H_c/H_d) upon increasing concentration, consistent with an increase in H-bonding and π–π stacking, respectively. These changes are consistent with formation of the same types of assemblies observed in the solid state and agree with the findings of **(±)-2a**. Fitting the change in amide N–H chemical shift to an isodesmic model allows determination of the elongation constant K_e (17 ± 1 M^{-1} at 298 K) for **(±)-1a** in chloroform (Figure 5b). This elongation constant is significantly less than that determined for **(±)-2a** (K_e = 63 ± 5 M^{-1} at 298 K).[15] DOSY NMR results also agree with a weaker supramolecular assembly for **(±)-1a** compared to **(±)-2a** (Table S3). In more polar $CDCl_3$, ^{1}H NMR spectra of **(±)-1a** show a time-average of the amide N–H and Ar–H as C_{ar}–C=O rotation is fast on the NMR timescale.

The same samples in cyclohexane-d_{12} show a pronounced broadening of all signals, including two individual amide N–H resonances. This is because the barrier to C_{ar}–C=O rotation becomes larger (and slow on the NMR timescale) due to intermolecular H-bonding (Figures S17–19). Invariance of the chemical shifts down to concentrations of 0.1 mM indicates persistent assemblies, consistent with our findings for **(±)-2a**. In contrast, solutions of non-assembling comparator **(±)-3** are molecularly dissolved at 30 mM in the same solvent (Figure S16). We can safely attribute the spectroscopic differences between **(±)-1a** and **(±)-3** to the solution phase self-assembly of **(±)-1a** in nonpolar solvents.

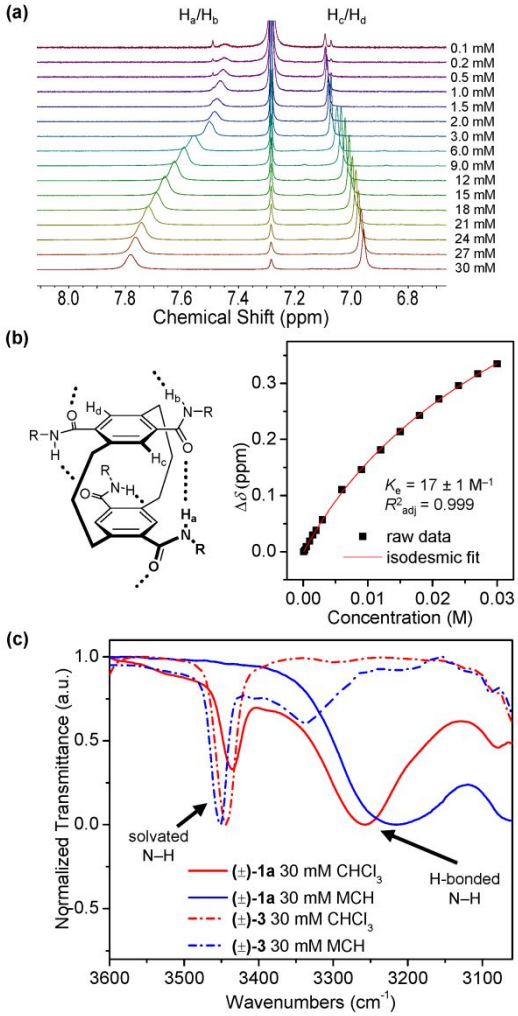

Figure 5. Variable concentration ^{1}H NMR (0.1–30 mM) of **(±)-1a** in $CDCl_3$ at 298 K (a). Nonlinear curve fitting of the change in amide N–H chemical shift to an isodesmic model (b). Overlaid and normalized solution FT-IR of **(±)-1a** and **(±)-3** (30 mM) in chloroform and methylcyclohexane (c).

Worth noting, in the synthesis of **(±)-1a–e**, small peaks not obviously corresponding to the product were observed in the aromatic region of the ^{1}H NMR spectrum in chloroform-*d* (Figure 5a). Upon dissolution in an H-bond competitive solvent (e.g., MeOD-d_4, DMSO-d_6 (Figure S14–15)) or heating to 100 °C in 1,1,2,2-tetrachloroethane-d_2, the small peaks disappeared into the baseline (Figure S11). These small peaks are believed to belong to metastable conformers of **(±)-1** due to the number of accessible conformers with reasonably high barriers to interconversion.

Infrared spectra of **(±)-1a** agree well with the results of the ^{1}H NMR analysis (Figure 5c). Solutions of **(±)-1a** in chloroform exhibit two N–H stretches: one solvated N–H stretch (3436 cm^{-1}) and one broad H-bonded N–H comprised of overlapping transannularly and intermolecularly H-bonded N–Hs. The H-bonded N–H peak shifts to lower energy (3265–3257 cm^{-1}) with an increase in concentration. Solutions of non-assembling comparator **(±)-3** in chloroform show only a single solvated N–H stretch (3444 cm^{-1}). Solutions of **(±)-1a** in a nonpolar solvent that favors stronger H-bonding, such as methylcyclohexane (MCH), show the single broad intermolecularly and transannularly H-bonded N–H stretch (3220 cm^{-1}) at concentrations as low as 0.3 mM. The lack of a solvated N–H stretch indicates that a negligible amount of the monomers is in the molecularly dissolved state. The

existence of few end-groups indicates relatively high degrees of polymerization under these conditions.

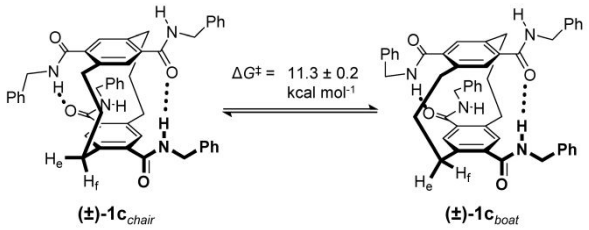

Figure 6. Barrier to interconversion between chair and boat conformers calculated from ^{1}H NMR line shape analysis of **(±)-1c** (26 mM in $CDCl_3$) at the coalescence temperature (258 K).

To examine the conformational dynamics associated with **(±)-1** (Figure 6), a low-temperature NMR study was performed. A solution of compound **(±)-1c** (26 mM in $CDCl_3$) was chosen to clearly analyze the line shape of the bridge protons on C1–3 and C10–12. At 298 K, the spectrum is simplified as *chair–boat* interconversion is fast on the NMR timescale. The line shape of the NMR signals corresponding to the two diastereotopic bridge protons H_e and H_f is slightly broadened compared to the other signals, indicating some slowed motion in the alkyl bridge (Figure S13). As the solution is cooled, these resonances become broadened until coalescence at 258 K, the same temperature reported for a CD_2Cl_2 solution of **[3.3]pCp**.[41] The interconversion of *boat* and *chair* conformations of **(±)-1c** at 221 K is slow compared to the NMR timescale, although the bridge resonances are still broadened, likely due to aggregation at low temperatures. The relative populations of *chair* and *boat* are difficult to determine (likely ca. 1:1 based on DFT computations, Table S1), but a determination of the *chair–boat* interconversion barrier from line shape analysis gives $\Delta G^{\ddagger} = 11.3 \pm 0.2$ kcal mol^{-1} at 258 K, which is consistent with the previously calculated values for **[3.3]pCp** of 12.0 kcal mol^{-1} at 258.2 K in CD_2Cl_2 and 11.7 ± 0.5 kcal mol^{-1} at 243.2 K in toluene-d_8.[40-41] The similar $\Delta G^{\ddagger}$ values for *chair–boat* interconversion in **[3.3]pCpTA** and **[3.3]pCp** indicates that the presence of

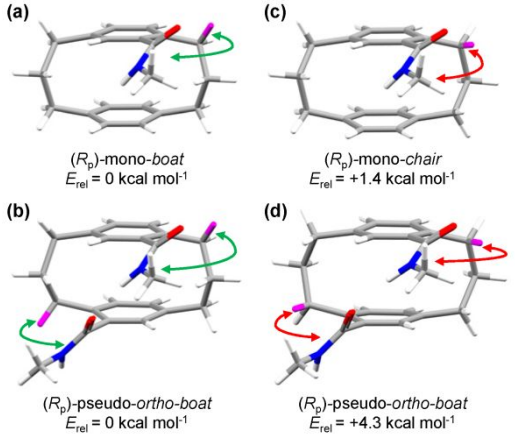

Figure 7. Optimized geometries and relative energies of some selected [3.3]pCp-5-monocarboxamide conformers and pseudo-*ortho*-[3.3]pCp-5,14-dicarboxamides shown with a central methylene pointing towards (a,b) and away (c,d) from amides engaged in transannular H-bonding. Results obtained from DFT calculations at the M06-2X/6-31+G* level of theory. Bridge hydrogen atoms involved in steric interactions colored purple; more costly and less costly interactions are labeled as green and red arrows, respectively.

transannular H-bonding does not significantly raise the barrier to *chair–boat* interconversion.

The effects of amide substitution on **[3.3]pCp** bridge conformation could be examined theoretically by gas-phase DFT calculations (M06-2X/6-31+G* level of theory) of **[3.3]pCp** mono- and bis-amide comparator molecules. A conformational search through a combination of *chair/boat* bridge conformers and amide conformers reveals a steric clash between the amides and the *ortho*-benzylic hydrogen of the alkyl bridge (Figure 7). This interaction is highest in energy when the central methylene bridge carbon is pointed away from the amides, forcing the hydrogen atom towards the amide substituents. Extrapolation of these results to **[3.3]pCpTA**, in which there is substitution at four *ortho* positions, means that there will always be at least two steric interactions with the alkyl bridge, slightly raising the ground state energy and lowering the barrier to *chair–boat* interconversion.

Assembly thermodynamics of **(±)-2a** have been characterized by variable temperature UV-Vis studies, but repeated attempts to study the assembly of **(±)-1a** by the same methods resulted in UV-Vis cooling curves that lacked clear isosbestic points (Figure S41). We believe this is due to the existence and assembly of both *chair* and *boat* monomers. This systematic change unfortunately precludes thermodynamic characterization by UV-Vis spectroscopy.

The reason **(±)-1** forms a weaker assembly than **(±)-2** is a result of the change in [n.n]paracyclophane structure and the supramolecular assembly it confers. This includes entropic effects associated with an increase in monomer dynamics for **(±)-1** compared to **(±)-2**, as well as steric clashes with the alkyl bridge, and larger amide dihedral angles to optimize transannular H-bonding. Initially, it was hypothesized that the increased electron-rich character in **[3.3]pCp**[20] could contribute to intermonomer repulsion upon cofacial assembly. Based on the similarity of intermolecular H-bond (N···O) distances of **(±)-1c** and **(±)-2b** in the crystal structures (~2.8 Å), the average hydrogen bond strength is expected to be nearly the same. The increase in amide dihedral angles in **(±)-1** as amides twist further out of the arene plane to optimize transannular H-bond distances, causes the π–π distances to increase (> 3.9 Å) so that they are outside the accepted range for π–π interactions. Therefore, repulsion of the more electron-rich π-decks in **(±)-1** is expected to be minor. The scissor motion in **(±)-1** will increase the number of energetically accessible conformations, leading to a decrease in the population of the conformation that is optimal for intermolecular association. This scissor motion of the bridge will also introduce destabilizing interactions to the amides (Figure 7), and further lower the barrier to amide rotation. Due to the greater rigidity of **(±)-2** compared to **(±)-1**, the monomer is more predisposed for self-complementary recognition and therefore assembly is more favorable.

The covalently fixed nature of these **[n.n]pCpTAs** ensures that the predisposed helical monomer does not change with assembly, allowing the association constant for self-recognition to stay the same regardless of assembly size (equal-K). In addition to the structural rationale, the *anti*- conformer could also be predicted to maintain a constant K_e due to the net-cancellation of assembly macrodipole and equivalent donor–acceptor H-bonding arrangement.

Due to the reversibility of the supramolecular polymerization, and the fast rotation of the C_{ar}–C=O bond in nonpolar solvents even in the presence of transannular H-bonding, supramolecular polymerization under thermodynamic control should result in pathway selection of one assembling species. Based on DFT calculations and macrodipole considerations, the isodesmic assembly of thus synthesized **[n.n]pCpTAs** is believed to correspond to the *anti*- conformer, which is consistent with prior computational investigations.[16] The barrier to rotation of the C_{ar}–C=O bond should increase as the polymer grows and interconversion would require breaking multiple H-bonds. This

"amide flipping" could still be possible, if very slow. Kinetic experiments are necessary to determine the effect of relative amide conformation on assembly on both short and long timescales.

CONCLUSIONS

In this work we have synthesized and characterized the second example of homochiral self-assembling paracyclophanes; **[3.3]pCpTA**. We have identified the mechanism of supramolecular polymerization for the two known self-assembling systems (**[2.2]pCpTA** and **[3.3]pCpTA**) as isodesmic and found that **[n.n]pCpTA** structure confers supramolecular structure and thermodynamics. The introduction of an additional bridge methylene provided insight into a structure–property relationship in **[n.n]pCpTAs** and revealed the consequences of **[n.n]pCpTA** structure and dynamics on supramolecular assembly.

As the size of the paracyclophane scaffold increases in **[3.3]pCpTA**, the accompanying decrease in strain energy, increase in conformational freedom, and increased deck-to-deck spacing when compared to **[2.2]pCpTA**, leads to a notable decrease in assembly strength for **[3.3]pCpTA**. This change is due to an increase in monomer entropy associated with the scissor motion of the **[3.3]pCp** bridge and enthalpic consequences associated with the amide dihedral angles required to accommodate transannular H-bonding across the larger **[3.3]pCp**.

The isodesmic self-assembly mechanism is relatively unique among other helical, H-bonding supramolecular polymers,[50-53] indicating that **[n.n]pCpTAs** can serve as a model system for further understanding structure–mechanism relationships in supramolecular polymers. The relative amide conformation (*syn*-and *anti*-) and its impact on the assembly mechanism and thermodynamics of these paracyclophanes, especially the role of the assembly macrodipole, remains of interest and is currently being explored.

EXPERIMENTAL SECTION

General Information. Reagents and solvents were purchased from commercial sources and used without further purification unless otherwise specified. THF, Et_2O, CH_2Cl_2, and DMF were degassed in 20 L drums and passed through two sequential purification columns (activated alumina; molecular sieves for DMF) under a positive argon atmosphere. Thin layer chromatography (TLC) was performed on SiO_2-60 F_{254} aluminum plates with visualization by UV light or staining. Flash column chromatography was performed using Silica gel technical grade, pore size 60 Å, 230−400 mesh particle size, 40−63 μm particle size from Sigma-Aldrich. 500 (125) MHz ^{1}H (^{13}C) NMR were recorded on an INOVA 500 spectrometer. Chemical shifts (δ) are given in parts per million (ppm) relative to TMS and referenced to residual protonated solvent purchased from Cambridge Isotope Laboratories, Inc. ($CDCl_3$: δ_H 7.26 ppm, δ_C 77.16 ppm; DMSO-d_6: δ_H 2.50 ppm, δ_C 39.52 ppm; acetone-d_6: δ_H 2.05 ppm, δ_C 29.84 ppm). Abbreviations used are s (singlet), d (doublet), t (triplet), q (quartet), quin (quintet), hp (heptet), b (broad), and m (multiplet). ESI-TOF-, APCI-TOF-, and DART-TOF-MS spectra were recorded on an Agilent 6210 TOF spectrometer with MassHunter software. EI-MS (70 eV) spectra were recorded on a Thermo Scientific DSQ MS after sample introduction via GC with data processing on Xcalibur software (accurate masses are calculated with the CernoBioscience MassWorks software). α,α'-Dibromo-*p*-xylene (**4**) was purchased from Alfa Aesar. 1,4-Bis[2-isocyano-2-(tolylsulfonyl)ethyl]benzene (TosMIC adduct **10**)[54] and 2-bromo-1,4-bis[2-isocyano-2-(tolylsulfonyl)ethyl]benzene (Br-TosMIC adduct **5**)[47] were synthesized according to literature procedures. [3.3]Paracyclophane was prepared by a known literature procedure involving macrocyclization of **4** and **10** in DMF.[46] Compounds **(±)-2a** and **(±)-2b** have been previously reported by our group.[15] Details of solution assembly studies, X-ray experimental, and computational studies can be found in the supporting information.

Synthesis of [3.3]paracyclophanes

(±)-5-Bromo[3.3]paracyclophane-2,11-dione (**(±)-12**). A procedure was adopted from the literature[47] as follows. A mixture of *n*-Bu_4NI (2.00 g, 5.41 mmol) dissolved in DCM (1 L), and NaOH (30 g, 0.8 mol) dissolved in H_2O (70 mL), was stirred in a 2 L round bottom flask and heated to reflux. To this mixture was added dropwise a mixture of α,α-dibromo-*p*-xylene (**4**) (2.33 g, 8.82 mmol) and Br-TosMIC adduct **5** (5.07 g, 8.82 mmol) in DCM (450 mL) over a period of 10 h, and the reflux was continued for another 10 h. The reaction mixture was cooled and the layers separated. The organic layer was washed with water (200 mL) and concentrated to a volume of ca. 100 mL. To this solution, concentrated HCl was added and the solution was stirred for 2 h at rt. The solution was diluted with water (200 mL) and DCM (200 mL). The organic layer was washed with brine, dried with $MgSO_4$, and evaporated to dryness. The crude reaction mixture was purified by column chromatography on silica using DCM as the eluent to yield **(±)-12** as a white solid (1.50 g, 48% yield). The product could be further purified by recrystallization from a mixture of DCM/hexanes. ^{1}H NMR (500 MHz, chloroform-*d*) δ 7.28 (d, J = 7.6 Hz, 1H), 7.08 (s, 1H), 6.96–6.88 (m, 2H), 6.86–6.79 (m, 3H), 4.22 (d, J = 13.4 Hz, 1H), 3.79 (d, J = 12.9 Hz, 1H), 3.76–3.60 (m, 6H), 3.53 (d, J = 13.3 Hz, 1H). ^{13}C{^{1}H} NMR (125 MHz, chloroform-*d*) δ 206.1, 205.4, 142.5, 137.3, 135.0, 134.9, 134.5, 131.7, 130.9, 130.1, 129.9, 129.4, 128.9, 125.9, 52.2, 51.8, 51.4, 51.2. IR (ATR) 1701 cm^{-1} (s). HRMS (DART) *m/z*: $[M+Na]^+$ calc'd for $C_{18}H_{15}BrO_2Na$: 365.0148, found 365.0150.

(±)-5-Bromo[3.3]paracyclophane (**(±)-6**). Compound **(±)-12** (1.5 g, 4.4 mmol) was added to a 100 mL 3-necked round bottom flask with a condenser, along with 50 mL of diethylene glycol, and 6.0 mL hydrazine hydrate (0.12 mol). The solution was heated to 130 °C for 2 h until all solids had dissolved. At this point, the solution was cooled to 100 °C and KOH (8.0 g, 0.14 mol) was added in one portion. The reflux condenser was left in until the solids dissolved, and then removed while the solution was heated at 130 °C for 1 h. The condenser was replaced and the solution was heated to 200 °C for 3 h. The solution was cooled to rt and poured into a 250 mL beaker with ice and extracted 3 times with DCM. Purification of the crude solid by column chromatography on silica with hexanes (R_f = 0.4) yielded **(±)-6** as a white powder (1.21 g, 86% yield). ^{1}H NMR (500 MHz, chloroform-*d*) δ 7.06 (d, J = 7.7 Hz, 1H), 6.93 (s, 1H), 6.86–6.55 (m, 6H), 3.10 (ddd, J = 13.1, 8.7, 3.1 Hz, 1H), 2.54 (m, 7H), 2.18–1.81 (m, 4H). ^{13}C{^{1}H} NMR (125 MHz, chloroform-*d*) δ 141.0, 138.6, 138.3, 137.2, 133.4, 132.3, 130.5, 129.6, 129.2, 128.4, 127.6, 124.5, 110.1, 36.0, 35.6, 35.5, 35.2, 29.9, 29.6, 27.4. MS (EI) *m/z*: $[M]^+$ calc'd for $C_{18}H_{19}Br$: 314.1, found: 314.2. ^{1}H NMR data was consistent with previously reported compound.[44,55-56]

(±)-5,8,14,17-Tetrabromo[3.3]paracyclophane (**(±)-7**). [3.3]Paracyclophane (80 mg, 0.33 mmol) and iodine (25 mg, 0.098 mmol, 1 crystal) were placed in a 2-necked round bottom flask equipped with an addition funnel and gas outlet, and covered with aluminum foil to exclude light. The flask was cooled to 0 °C in an ice–water bath and bromine (5 mL, 0.1 mol) was slowly added over 3 h via addition funnel. Emitted hydrogen bromide gas was trapped in cold saturated $NaHCO_3$ solution. The reaction mixture was stirred at rt under dry air, and TLC was taken to monitor the reaction progress. After 6 h (from the start of Br_2 addition), the reaction was completed. Residual bromine was evaporated with agitation from the reaction mixture to leave a red powder. The powder was dissolved in dichloromethane and washed with 10%

$Na_2S_2O_3$ solution and brine. After drying over Na_2SO_4, the solvent was removed in vacuo, and the crude product was purified by repeated silica gel column chromatography (100% hexanes, R_f = 0.50) to yield a white solid (97 mg, 52% yield). 5,6,17,18-Tetrabromo[3.3]paracyclophane was isolated as a less polar side product (R_f = 0.45). ^{1}H NMR (500 MHz, chloroform-*d*): δ 7.29 (s, 4H), 2.99 (dt, J = 14.4, 6.0 Hz, 4H), 2.58 (dt, J = 14.4, 6.4 Hz, 4H), 2.19 (p, J = 6.1 Hz, 4H). ^{13}C{^{1}H} NMR (125 MHz, chloroform-*d*): δ 139.4, 133.5, 124.4, 34.6, 23.9. HRMS (DART) *m/z*: $[M]^+$ calc'd for $C_{18}H_{16}Br_4$: 551.7940, found 551.7946. **(±)-7** could be synthesized following the same procedure from **(±)-6** with a slight improvement in yield.

(±)-5,8,14,17-Tetracarboxy[3.3]paracyclophane (**(±)-8**). Compound **(±)-7** (125 mg, 0.226 mmol) was placed in a flame-dried 2-neck round bottom flask under argon atmosphere and dissolved in THF (3 mL). The solution was cooled to –78 °C with a dry ice–acetone bath and a 1.7 M solution of *t*-butyllithium in pentane (1.60 mL, 2.71 mmol) was added slowly to the reaction mixture. The reaction mixture was stirred for 20 min, then CO_2 (16 g, 0.36 mol) was bubbled through the solution via a long needle with stirring until all the gas was consumed. The reaction mixture warmed to rt and dissolved in 10% $NaHCO_3$ and then acidified with concentrated HCl. A white precipitate was collected through filtration and the mother liquor was extracted with ethyl acetate. The organic layer was separated, dried with Na_2SO_4, and the solvent was removed under reduced pressure. The white precipitate was dissolved in ethyl acetate and the ethyl acetate solutions were combined and evaporated onto celite. The product could be further purified with column chromatography on silica gel (gradient of 90% hexanes:10% isopropanol with 1% trifluoroacetic acid to 85% hexanes:15% isopropanol with 1% trifluoroacetic acid) (R_f = 0.1) to yield **(±)-8** as a white solid (83 mg, 87% yield) ^{1}H NMR (500 MHz, acetone-d_6): δ 12.88 (br, 4H), 7.37 (s, 4H), 3.59 (dt, J = 14.1, 6.1 Hz, 4H), 2.54 (dt, J = 14.1, 6.0 Hz, 4H), 2.06 (p, J = 6.1 Hz, 4H). ^{13}C{^{1}H} NMR (125 MHz, acetone) δ 168.8, 141.3, 134.0, 133.9, 33.1, 29.1. HRMS (DART) *m/z*: $[M-H]^-$ calc'd for $C_{22}H_{19}O_8$: 411.1085, found 411.1074.

(±)-5,8,14,17-Tetra(n-hexyl)amide[3.3]paracyclophane (**(±)-1a**). Oxalyl chloride (0.090 mL, 1.0 mmol) was added to a solution of **(±)-8** (73 mg, 0.18 mmol) in DCM (5 mL). A catalytic amount of DMF (1 drop) was added and the mixture was stirred at rt for 2 h. Then solvent and unreacted oxalyl chloride were removed in vacuo. The resulting acid chloride intermediate was dissolved in DCM (5 mL). After cooling the solution to 0 °C, *n*-hexylamine (0.12 mL, 0.88 mmol) and *N*,*N*-diisopropylethylamine (DIPEA) (0.15 mL, 0.88 mmol) were added dropwise at 0 °C and the reaction mixture was allowed to warm to rt over 2 h. The reaction mixture was stirred overnight and then diluted with DCM and washed with 2 N HCl (2 × 10 mL), H_2O, and brine. The organic layer was separated, dried with $MgSO_4$, filtered, and the solvent was removed under reduced pressure. The product was further purified by silica gel chromatography (10–50% ethyl acetate in hexanes) and was obtained as a near white solid (30 mg, 22% yield). Further recrystallization by slow cooling a DMF/H_2O solution yielded shiny white crystals. ^{1}H NMR (500 MHz, chloroform-*d*): δ 7.68 (br s, 4H), 7.01 (s, 4H), 3.45 (m, 8H), 3.11 (br s, 4H), 2.55 (br s, 4H), 1.94 (p, J = 5.5 Hz, 4H), 1.68 (m, 4H), 1.44 (m, 4H), 1.38 (m, 8H), 0.92 (t, J = 7.0 Hz, 4H). ^{13}C{^{1}H} NMR (125 MHz, $CDCl_3$): δ 170.3, 137.4, 137.0, 129.5, 40.1, 31.7, 29.9, 29.5, 27.9, 27.0, 22.8, 14.2. HRMS (DART) *m/z*: $[M+H]^+$ calc'd for $C_{46}H_{73}N_4O_4$: 745.5626, found 745.5633.

(±)-5,8,14,17-Tetra(n-propyl)amide[3.3]paracyclophane (**(±)-1b**). Synthesized in the same way as **(±)-1a** using **(±)-8** (21 mg, 0.044 mmol), oxalyl chloride (0.048 mL, 0.58 mmol), *n*-propylamine (0.10 mL, 1.2 mmol), and *N*,*N*-diisopropylethylamine (DIPEA) (0.10 mL, 0.57 mmol). The product was further purified by silica gel chromatography (70–90% ethyl acetate in hexanes) and was obtained as a white solid (10 mg, 41% yield). Crystallization by slow evaporation from MeOH or EtOH, or by slow cooling from DMF/H_2O, yielded thin needles of insufficient quality for single-crystal X-ray diffraction. ^{1}H NMR (500 MHz, chloroform-*d*): δ 7.68 (br s, 4H), 6.98 (s, 4H), 3.41 (m, 8H), 3.11 (br s, 4H), 2.52 (br s, 4H), 1.93 (p, J = 5.7 Hz, 4H), 1.71 (m, 4H), 1.03 (t, J = 7.3 Hz, 4H). ^{13}C{^{1}H} NMR (125 MHz, $CDCl_3$): δ 170.2, 137.2, 136.8, 129.4, 41.7, 29.7 27.8, 22.7, 11.7. HRMS (DART) *m/z*: $[M+H]^+$ calc'd for $C_{34}H_{49}N_4O_4$: 577.3754, found 577.3772.

(±)-5,8,14,17-Tetrabenzylamide[3.3]paracyclophane (**(±)-1c**). Synthesized in the same way as **(±)-1a** using **(±)-8** (67 mg, 0.16 mmol), oxalyl chloride (0.20 mL, 2.7 mmol), benzylamine (0.50 mL, 4.6 mmol), and *N*,*N*-diisopropylethylamine (DIPEA) (0.10 mL, 0.57 mmol). The product was further purified by silica gel chromatography (70% ethyl acetate in hexanes) and was obtained as a white solid (29 mg, 23% yield). Crystallization by slow evaporation from ethyl acetate/ethanol furnished colorless crystals suitable for single-crystal X-ray diffraction. ^{1}H NMR (500 MHz, chloroform-*d*) δ 7.99 (br s, 4H), 7.42–7.22 (m, 5H), 6.89 (s, 4H), 4.67–4.49 (m, 8H), 3.00 (br s, 4H), 2.37 (br s, 4H), 1.73 (br s, 4H). ^{13}C{^{1}H} NMR (125 MHz, $CDCl_3$): δ 170.0, 138.8, 136.8, 136.7, 129.2, 128.6, 128.4, 127.4, 44.0, 33.0, 27.7. HRMS (ESI) *m/z*: $[M+H]^+$ calc'd for $C_{50}H_{49}N_4O_4$: 769.3748, found: 769.3746.

(±)-5,8,14,17-Tetraphenylamide[3.3]paracyclophane (**(±)-1d**). Synthesized in the same way as **(±)-1a** using **(±)-8** (25 mg, 0.060 mmol), oxalyl chloride (0.05 mL, 0.68 mmol), aniline (1.0 mL, 10 mmol), and *N*,*N*-diisopropylethylamine (DIPEA) (0.10 mL, 0.57 mmol). The product was further purified by silica gel chromatography (0–10% methanol in DCM) and was obtained as an off-white solid (13 mg, 23% yield). Further purification by recrystallization from ethyl acetate-ethanol yielded pure **(±)-1d**. ^{1}H NMR (500 MHz, chloroform-*d*) δ 10.57 (br s, 4H), 8.00–7.90 (m, 8H), 7.37 (t, J = 7.9 Hz, 8H), 7.19–7.09 (m, 4H), 6.85 (s, 4H), 3.14–2.81 (br s, 4H), 2.32 (br s, 4H), 1.81–1.62 (m, 4H). ^{13}C{^{1}H} NMR (125 MHz, chloroform-*d*) δ 168.6, 139.1, 137.2, 137.0, 129.6, 129.2 124.5, 120.1, 33.4, 29.9, 27.9. HRMS (ESI) *m/z*: $[M+H]^+$ calc'd for $C_{46}H_{41}N_4O_4$: 713.3122, found: 713.3121.

(±)-5,8,14,17-Tetraethylamide[3.3]paracyclophane (**(±)-1e**). Synthesized in the same way as **(±)-1a** using **(±)-8** (12 mg, 0.029 mmol), oxalyl chloride (0.02 mL, 0.3 mmol), ethylamine 2.0 M in THF (1.0 mL, 2.0 mmol), and *N*,*N*-diisopropylethylamine (DIPEA) (0.10 mL, 0.57 mmol). The product was further purified by silica gel chromatography (0–10% methanol in DCM) and was obtained as an off-white solid (5 mg, 33% yield). Further purification by recrystallization from methanol yielded pure **(±)-1e** as small colorless needles. ^{1}H NMR (500 MHz, chloroform-*d*) δ 7.50 (br s, 4H), 7.06 (s, 4H), 3.52 (m, 8H), 3.16 (br s, 4H), 2.58 (br s, 4H), 1.97 (br s, 4H), 1.32 (t, J = 7.3 Hz, 12H). ^{13}C{^{1}H} NMR (125 MHz, chloroform-*d*) δ 170.4, 137.4, 137.0, 129.5, 41.9, 29.9, 27.9, 22.9, 11.9. HRMS (ESI) *m/z*: $[M+H]^+$ calc'd for $C_{30}H_{41}N_4O_4$: 521.3122, found: 521.3107.

(±)-5-Carboxy[3.3]paracyclophane (**(±)-9**). This compound was synthesized in the same way as **(±)-8**, with **(±)-6** (17 mg, 0.54 mmol), *t*-BuLi (1.5 M in hexanes, 2 mL, 3 mmol), and CO_2 (16 g, 0.36 mol) to yield a white powder (128 mg, 84% yield). Silica gel chromatography (70% ethyl acetate in hexanes) had significant coelution with pivalic acid by-product so the product was used without further purification. ^{1}H NMR (400 MHz, chloroform-*d*) δ 7.56–7.44 (s, 1H), 6.87–6.62 (m, 6H), 3.80 (m, 1H), 3.08–2.45 (m, 7H), 2.31–1.99 (m, 4H). ^{13}C{^{1}H} NMR (100 MHz, chloroform-*d*) δ 173.9, 142. 1, 139.2, 138.7, 138.5, 138.3, 134.9, 133.6, 132.3, 130.6, 129.7, 129.2, 127.4, 38.8, 36.1, 36.0, 35.6, 35.5, 34.9, 29.9, 29.6, 29.0. HRMS (ESI) *m/z*: $[M–H]^–$ calc'd for $C_{19}H_{19}O_2$:

279.1391, found 279.1403. ^{1}H NMR and ^{13}C NMR are consistent with literature values.[57]

(±)-5-(n-Hexyl)amide[3.3]paracyclophane (**(±)-3**). This compound was synthesized in the same way as **(±)-1a** with **(±)-9** (256 mg, 0.913 mmol), oxalyl chloride (0.29 mL, 3.6 mmol), and DCM (20 mL). The product was purified by silica gel chromatography (30% ethyl acetate in hexanes) to give a white powder (114 mg, 34% yield). ^{1}H NMR (400 MHz, chloroform-*d*) δ 6.91–6.85 (s, 1H), 6.84–6.57 (m, 6H), 5.64 (br s, 1H), 3.46 (ddd, J = 12.8, 7.1, 5.7 Hz, 2H), 3.26 (ddd, J = 14.2, 8.7, 2.9 Hz, 1H), 3.00–2.48 (m, 7H), 2.29–1.88 (m, 4H), 1.64 (q, J = 7.3 Hz, 3H), 1.51–1.29 (m, 6H), 1.05–0.84 (m, 3H). ^{13}C{^{1}H} NMR (100 MHz, chloroform-*d*) δ 170.4, 139.1, 138.9, 138.4, 136.7, 135.1, 132.5, 131.8, 130.0, 129.7, 129.3, 129.2, 127.7, 40.0, 36.1, 35.7, 35.6, 33.4, 31.7, 29.9, 29.7, 28.9, 26.9, 22.8, 14.2. HRMS (ESI) *m/z*: $[M+H]^+$ calc'd for $C_{25}H_{34}NO$: 364.2635, found 364.2650.

ASSOCIATED CONTENT

The Supporting Information is available free of charge on the ACS Publications website at DOI: Detailed synthetic schemes, ^{1}H and ^{13}C NMR spectra, NMR assembly studies, IR spectra, UV-Vis spectra, computational details (including coordinates of optimized structures), and X-ray crystallographic data for **(±)-1c**.

AUTHOR INFORMATION

Corresponding Author

*E-mail: castellano@chem.ufl.edu

ORCID
Ronald K. Castellano: 0000-0003-4322-9932
Will R. Henderson: 0000-0003-4791-3184
Yu Zhu: 0000-0001-6745-0389
Danielle E. Fagnani: 0000-0003-3373-4265

ACKNOWLEDGMENT

Acknowledgement is made to the Donors of the *American Chemical Society Petroleum Research Fund* for support of this research (PRF #56665-ND4). K. A. A. wishes to acknowledge the *National Science Foundation* and the University of Florida for funding of the purchase of the X-ray equipment. We acknowledge University of Florida (UF) Research Computing for providing computational resources and support that have contributed to the research results reported in this publication (https://www.rc.ufl.edu). The mass spectrometric data were obtained by the UF Department of Chemistry Mass Spectrometry Research and Education Center supported, in part, by the National Institutes of Health (NIH S10 OD021758-01A1). We also would like to thank Dr. Ion Ghiviriga for 2D-NMR assistance in assigning the structure of **(±)-7**.

REFERENCES

1. Yang, L.; Tan, X.; Wang, Z.; Zhang, X., Supramolecular Polymers: Historical Development, Preparation, Characterization, and Functions. *Chem. Rev.* **2015**, *115*, 7196-7239.
2. De Greef, T. F. A.; Smulders, M. M. J.; Wolffs, M.; Schenning, A. P. H. J.; Sijbesma, R. P.; Meijer, E. W., Supramolecular Polymerization. *Chem. Rev.* **2009**, *109*, 5687-5754.
3. Stals, P. J. M.; Everts, J. C.; de Bruijn, R.; Filot, I. A. W.; Smulders, M. M. J.; Martín-Rapún, R.; Pidko, E. A.; de Greef, T. F. A.; Palmans, A. R. A.; Meijer, E. W., Dynamic Supramolecular Polymers Based on Benzene-1,3,5-tricarboxamides: The Influence of Amide Connectivity on Aggregate Stability and Amplification of Chirality. *Chem. Eur. J.* **2010**, *16*, 810-821.
4. Philips, D. S.; Kartha, K. K.; Politi, A. T.; Krüger, T.; Albuquerque, R. Q.; Fernández, G., Interplay between H-Bonding and Preorganization in the Evolution of Self-Assembled Systems. *Angew. Chem. Int. Ed.* **2019**, *58*, 4732-4736.
5. Buendía, J.; Calbo, J.; García, F.; Aragó, J.; Viruela, P. M.; Ortí, E.; Sánchez, L., Helical supramolecular polymerization of C_3-symmetric amides and retroamides: on the origin of cooperativity and handedness. *Chem. Commun.* **2016**, *52*, 6907-6910.
6. Kaiser, T. E.; Stepanenko, V.; Würthner, F., Fluorescent J-Aggregates of Core-Substituted Perylene Bisimides: Studies on Structure−Property Relationship, Nucleation−Elongation Mechanism, and Sergeants-and-Soldiers Principle. *J. Am. Chem. Soc.* **2009**, *131*, 6719-6732.
7. Kulkarni, C.; Meijer, E. W.; Palmans, A. R. A., Cooperativity Scale: A Structure–Mechanism Correlation in the Self-Assembly of Benzene-1,3,5-tricarboxamides. *Acc. Chem. Res.* **2017**, *50*, 1928-1936.
8. Casellas, N. M.; Pujals, S.; Bochicchio, D.; Pavan, G. M.; Torres, T.; Albertazzi, L.; García-Iglesias, M., From isodesmic to highly cooperative: reverting the supramolecular polymerization mechanism in water by fine monomer design. *Chem. Commun.* **2018**, *54*, 4112-4115.
9. Dorca, Y.; Matern, J.; Fernández, G.; Sánchez, L., C_3-symmetrical π-Scaffolds: Useful Building Blocks to Construct Helical Supramolecular Polymers. *Israel Journal of Chemistry* **2019**, *0*.
10. Cantekin, S.; de Greef, T. F. A.; Palmans, A. R. A., Benzene-1,3,5-tricarboxamide: a versatile ordering moiety for supramolecular chemistry. *Chem. Soc. Rev.* **2012**, *41*, 6125-6137.
11. Sun, H.; Hunter, C. A.; Llamas, E. M., The flexibility–complementarity dichotomy in receptor–ligand interactions. *Chem. Sci.* **2015**, *6*, 1444–1453.
12. Adelizzi, B.; Filot, I. A. W.; Palmans, A. R. A.; Meijer, E. W., Unravelling the Pathway Complexity in Conformationally Flexible *N*-Centered Triarylamine Trisamides. *Chem. Eur. J.* **2017**, *23*, 6103-6110.
13. Berrocal, J. A.; Di Meo, F.; García-Iglesias, M.; Gosens, R. P. J.; Meijer, E. W.; Linares, M.; Palmans, A. R. A., Consequences of conformational flexibility in hydrogen-bond-driven self-assembly processes. *Chem. Commun.* **2016**, *52*, 10870-10873.
14. Yamauchi, M.; Adhikari, B.; Prabhu, D. D.; Lin, X.; Karatsu, T.; Ohba, T.; Shimizu, N.; Takagi, H.; Haruki, R.; Adachi, S.-i.; Kajitani, T.; Fukushima, T.; Yagai, S., Supramolecular Polymerization of Supermacrocycles: Effect of Molecular Conformations on Kinetics and Morphology. *Chem. Eur. J.* **2017**, *23*, 5270-5280.
15. Fagnani, D. E.; Meese Jr., M. J.; Abboud, K. A.; Castellano, R. K., Homochiral [2.2]Paracyclophane Self-Assembly Promoted by Transannular Hydrogen Bonding. *Angew. Chem. Int. Ed.* **2016**, *55*, 10726-10731.
16. Korlepara, D. B.; Henderson, W. R.; Castellano, R. K.; Balasubramanian, S., Differentiating the mechanism of self-assembly in supramolecular polymers through computation. *Chem. Commun.* **2019**, *55*, 3773-3776.
17. Henderson, W. R.; Fagnani, D. E.; Grolms, J.; Abboud, K. A.; Castellano, R. K., Transannular Hydrogen Bonding in Planar-Chiral [2.2]Paracyclophane-Bisamides. *Helv. Chim. Acta* **2019**, *102*, e1900047.
18. Starikova, Z. A.; Fedyanin, I. V.; Antipin, M. Y., Conformational rigidity and flexibility of the paracyclophane skeleton in substituted [2.2]paracyclophanes. *Russ. Chem. Bull.* **2004**, *53*, 1779–1805.
19. Singer, L. A.; Cram, D. J., Macro Rings. XXVII. Transannular Substituent Effects in π-π-Complexes of Paracyclophanes. *J. Am. Chem. Soc.* **1963**, *85*, 1080–1084.
20. Sheehan, M.; Cram, D. J., Macro rings. XL. Transannular interactions in the tetracyanoethylene complexes of [3.3]paracyclophane and derivatives. *J. Am. Chem. Soc.* **1969**, *91*, 3553-3558.
21. Schanne, L.; Staab, H. A., Complexation of electron donor-acceptor [2.2] paracyclophanes with tetracyanoethylene (TCNE). *Tetrahedron Lett.* **1984**, *25*, 1721–1724.
22. Staab, H. A.; Wahl, P.; Kay, K.-Y., Electron Donor-Acceptor Compounds, 45 Syntheses of [2.2]-, [3.3]-, and [4.4]Paracyclophanes with 1,2,4,5-Tetracyanobenzene Units as Electron Acceptors. *Chem. Ber.* **1987**, *120*, 541-549.
23. Misumi, S.; Otsubo, T., Chemistry of multilayered cyclophanes. *Acc. Chem. Res.* **1978**, *11*, 251-256.

24. Shibahara, M.; Watanabe, M.; Yuan, C.; Goto, K.; Shinmyozu, T., Structural properties of charge-transfer complexes of multilayered [3.3]paracyclophanes. *Tetrahedron Lett.* **2011**, *52*, 3371-3375.
25. Fujitsuka, M.; Tojo, S.; Shibahara, M.; Watanabe, M.; Shinmyozu, T.; Majima, T., Delocalization of Positive Charge in π-Stacked Multi-benzene Rings in Multilayered Cyclophanes. *J. Phys. Chem. A* **2011**, *115*, 741-746.
26. Watanabe, M.; Goto, K.; Shibahara, M.; Shinmyozu, T., Synthesis, Structure, and Electronic and Photophysical Properties of Two- and Three-Layered [3.3]Paracyclophane-Based Donor−Acceptor Systems. *J. Org. Chem.* **2010**, *75*, 6104-6114.
27. Fujitsuka, M.; Miyazaki, T.; Lu, C.; Shinmyozu, T.; Majima, T., Multistep Electron Transfer Systems Containing [2.2]- or [3.3]Paracyclophane. *J. Phys. Chem. A* **2016**, *120*, 1184-1189.
28. Miyazaki, T.; Shibahara, M.; Fujishige, J.-i.; Watanabe, M.; Goto, K.; Shinmyozu, T., Synthesis and Electronic and Photophysical Properties of [2.2]- and [3.3]Paracyclophane-Based Donor–Donor'–Acceptor Triads. *J. Org. Chem.* **2014**, *79*, 11440-11453.
29. Kovač, B.; Allan, M.; Heilbronner, E., 'Through Space' and 'Through Bond' Interactions in [2.2]Cyclopanes; the Assignment of their Photoelectron Spectra. *Helv. Chim. Acta* **1981**, *64*, 430–448.
30. Shieh, C.-F.; McNally, D.; Boyd, R. H., The heats of combustion and strain energies of some cyclophanes. *Tetrahedron* **1969**, *25*, 3653-3665.
31. Szymański, S.; Dodziuk, H.; Pietrzak, M.; Jaźwiński, J.; Demissie, T. B.; Hopf, H., Dynamics of [n.3]paracyclophanes (n = 2–4) as studied by NMR. Obtaining separate Arrhenius parameters for two dynamic processes in [4.3]paracyclophane. *J. Phys. Org. Chem.* **2013**, *26*, 596-600.
32. Henseler, D.; Hohlneicher, G., Comment on "Distinctive Normal Harmonic Vibrations of [2.2]Paracyclophane". *J. Phys. Chem. A* **1999**, *103*, 1160–1161.
33. Walden, S. E.; Glatzhofer, D. T., Distinctive Normal Harmonic Vibrations of [2.2]Paracyclophane. *J. Phys. Chem. A* **1997**, *101*, 8233-8241.
34. Walden, S. E.; Glatzhofer, D. T., Reply to Comment on "Distinctive Normal Harmonic Vibrations of [2.2]Paracyclophane". *J. Phys. Chem. A* **1999**, *103*, 1162–1163.
35. Grimme, S., On the Importance of Electron Correlation Effects for the π–π Interactions in Cyclophanes. *Chem. Eur. J.* **2004**, *10*, 3423–3429.
36. Dodziuk, H.; Szymański, S.; Jaźwiński, J.; Ostrowski, M.; Demissie, T. B.; Ruud, K.; Kuś, P.; Hopf, H.; Lin, S.-T., Structure and NMR Spectra of Some [2.2]Paracyclophanes. The Dilemma of [2.2]Paracyclophane Symmetry. *J. Phys. Chem. A* **2011**, *115*, 10638-10649.
37. Bachrach, S. M., DFT Study of [2.2]-, [3.3]-, and [4.4]Paracyclophanes: Strain Energy, Conformations, and Rotational Barriers. *J. Phys. Chem. A* **2011**, *115*, 2396-2401.
38. Wolf, H.; Leusser, D.; Mads , R. V. J.; Herbst-Irmer, R.; Chen, Y.-S.; Scheidt, E.-W.; Scherer, W.; Iversen, B. B.; Stalke, D., Phase Transition of [2,2]-Paracyclophane – An End to an Apparently Endless Story. *Chem. Eur. J.* **2014**, *20*, 7048-7053.
39. Dodziuk, H.; Szymański, S.; Jaźwiński, J.; Marchwiany, M. E.; Hopf, H., Structure and Dynamics of [3.3]Paracyclophane As Studied by Nuclear Magnetic Resonance and Density Functional Theory Calculations. *J. Phys. Chem. A* **2010**, *114*, 10467-10473.
40. Anet, F. A. L.; Brown, M. A., Nuclear magnetic resonance studies of conformation and ring inversion in the [3.3]paracyclophane system. *J. Am. Chem. Soc.* **1969**, *91*, 2389–2391.
41. Sako, K.; Meno, T.; Shinmyozu, T.; Inazu, T.; Takemura, H., Conformational Analysis of [3.3]Paracyclophane. *Chem. Ber.* **1990**, *123*, 639–642.
42. Sorrenti, A.; Leira-Iglesias, J.; Markvoort, A. J.; de Greef, T. F. A.; Hermans, T. M., Non-equilibrium supramolecular polymerization. *Chem. Soc. Rev.* **2017**, *46*, 5476-5490.
43. Pechlivanidis, Z.; Hopf, H.; Ernst, L., Paracyclophanes: Extending the Bridges. Synthesis. *Eur. J. Org. Chem.* **2009**, *2009*, 223-237.
44. Tetsuo, O.; Hisanori, H.; Yosuke, K.; Soichi, M., Layered Compounds. LXIII. Bromination of Double- and Triple-layered Paracyclophanes. *Bull. Chem. Soc. Jpn.* **1980**, *53*, 1677-1682.
45. Kotha, S.; Shirbhate, M. E.; Waghule, G. T., Selected synthetic strategies to cyclophanes. *Beilstein J. Org. Chem.* **2015**, *11*, 1274-1331.
46. Matsuda-Sentou, W.; Shinmyozu, T., A Synthetic and Structural Study of 17,18-Dicyano[32](1,6)cyclooctatetraen(1,4)cyclophane Generated by Photolysis of [32](1,4)Barrelenophane. *Eur. J. Org. Chem.* **2000**, *2000*, 3195–3203.
47. Shibahara, M.; Watanabe, M.; Miyazaki, T.; Goto, K.; Matsumoto, T.; Shinmyozu, T., Synthesis of Dibromo[3.3]paracyclophanes. *Synthesis* **2016**, *48*, 1197-1201.
48. Reich, H. J.; Cram, D. J., Macro rings. XXXVII. Multiple electrophilic substitution reactions of [2.2]paracyclophanes and interconversions of polysubstituted derivatives. *J. Am. Chem. Soc.* **1969**, *91*, 3527-3533.
49. Tian, M.; Furuki, M.; Iwasa, I.; Sato, Y.; Pu, L. S.; Tatsuura, S., Search for Squaraine Derivatives That Can Be Sublimed without Thermal Decomposition. *J. Phys. Chem. B* **2002**, *106*, 4370-4376.
50. Smulders, M. M.; Schenning, A. P.; Meijer, E., Insight into the mechanisms of cooperative self-assembly: The "sergeants-and-soldiers" principle of chiral and achiral C_3-symmetrical discotic triamides. *J. Am. Chem. Soc.* **2008**, *130*, 606–611.
51. Stals, P. J. M.; Everts, J. C.; de Bruijn, R.; Filot, I. A. W.; Smulders, M. M. J.; Martin-Rapun, R.; Pidko, E. A.; de Greef, T. F. A.; Palmans, A. R. A.; Meijer, E. W., Dynamic Supramolecular Polymers Based on Benzene-1,3,5-tricarboxamides: The Influence of Amide Connectivity on Aggregate Stability and Amplification of Chirality. *Chem. Eur. J.* **2010**, *16*, 810–821.
52. Wang, F.; Gillissen, M. A. J.; Stals, P. J. M.; Palmans, A. R. A.; Meijer, E. W., Hydrogen Bonding Directed Supramolecular Polymerisation of Oligo(Phenylene-Ethynylene)s: Cooperative Mechanism, Core Symmetry Effect and Chiral Amplification. *Chem. Eur. J.* **2012**, *18*, 11761–11770.
53. Ogi, S.; Stepanenko, V.; Sugiyasu, K.; Takeuchi, M.; Würthner, F., Mechanism of Self-Assembly Process and Seeded Supramolecular Polymerization of Perylene Bisimide Organogelator. *J. Am. Chem. Soc.* **2015**, *137*, 3300-3307.
54. Sasaki, H.; Kitagawa, T., Synthesis of [3n]Cyclophanes and Related Compounds by Alkylation of Tosylmethyl Isocyanide with Bis (bromomethyl) benzenes. *Chem. Pharm. Bull.* **1983**, *31*, 2868–2878.
55. Chiu, Y.-H.; Shibahara, M.; Huang, R.-Y.; Watanabe, M.; Wang, Z.-S.; Hsiao, Y.-J.; Chang, B.-F.; Chiang, T.-H.; Chang, Y. J., Triphenylamine derivatives and the lithium-ion capture of [3.3]cyclophane used in organic dye-sensitized solar cells. *Dyes and Pigments* **2017**, *136*, 761–772.
56. Sheehan, M.; Cram, D. J., Macro rings. XXXIX. Syntheses and spectral properties of the aromatic monosubstituted derivatives of [3.3]paracyclophane. *J. Am. Chem. Soc.* **1969**, *91*, 3544–3552.
57. Pechlivanidis, Z.; Hopf, H.; Grunenberg, J.; Ernst, L., Paracyclophanes: Extending the Bridges. Reactions. *Eur. J. Org. Chem.* **2009**, *2009*, 238-252.

TOC Graphic:

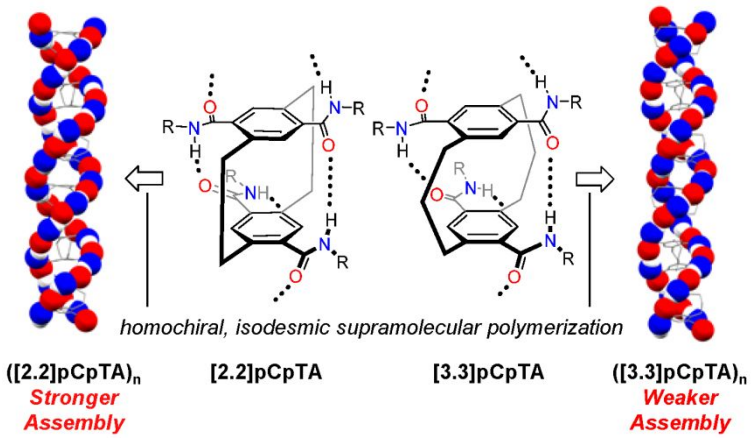
homochiral, isodesmic supramolecular polymerization
([2.2]pCpTA)n
Stronger
Assembly
[2.2]pCpTA
[3.3]pCpTA
([3.3]pCpTA)n
Weaker
Assembly